19th Australasian Fluid Mechanics Conference
Melbourne, Australia
8-11 December 2014

A Modeling and Simulation Framework for Transonic Flutter Analysis

K. L. Lai[1], and K. -Y. Lum[2]

[1]Temasek Laboratories
National University of Singapore, Singapore

[2]Department of Electrical Engineering
National Chi Nan University, Puli, Taiwan

Abstract

The paper presents an approach for flutter prediction using a combination of full-order computational aeroelastic (CAE) techniques and reduced-order modeling (ROM) methods. The aeroelastic equations of motion are resolved by using CAE to obtain time-domain aeroelastic responses, upon which ROM is applied to obtain an aeroelastic reduced-order model in discrete-time, state-space format. The resulting closed-loop aeroelastic model is thus analysed for Hopf bifurcation to predict the flutter boundaries. The present approach predicts flutter boundaries much faster than aeroelasticity simulation, lending it a practical engineering tool. For application and verification of the method, the benchmark transonic aeroelastic of AGARD 445.6 wing will be considered. Results show that the present approach predicts accuately the flutter boundaries.

Introduction

Aerodynamic flutter, an aeroelastic phenomenon caused by closed-loop interaction between aerodynamic and structural dynamic, constrains and even poses danger to the operation of aircraft. Flutter prediction is one important process in aircraft design. As an alternative to flight tests, computational aeroelasticity (CAE) has become a reliable tool for flutter analysis. Both linear unsteady aerodynamics and nonlinear high-level CFD methods have been developed and applied in CAE. When aerodynamic nonlinearities such as transonic flutter, shock waves, and high-angle-of-attack problem, the latter are the only methods capable of dealing with the problems.

Because of the high computational cost incurred by full-order CAE computation, its use for mapping out the flutter boundaries in the entire flight envelop will lead to excessively long turnaround time. To this connection reduced-order modeling (ROM) techniques have been applied in aeroelastic analysis. ROM can reduce the computational time by several orders of magnitude. In general, a reduced-order aerodynamic model is obtained and deployed in lieu of the full-order unsteady flow solver. Generation of ROM involves two functional steps – generation of training data, and calculation of reduced-order model. Both experimental results and computational results can be used as ROM training data. The system is subjected to prescribed perturbation[1, 2, 4, 9, 10], and aeroelastic responses are measured and taken as ROM training data. A number of different techniques have been developed for calulating reduced-order models. These include Eigenvalue (Modal) Truncation, Balanced Model Reduction, Karhunen-Loeve or Singular Value Decomposition, System Identification methods, Fourier Series methods, and Hybrid techniques. Dowell and Hall [3] presents a comprehensive review of recent works. Noor [8] gives some early examples of model reduction techniques.

In the present work CFD results are used as ROM training data. Full-order CAE simulations are performed to compute the unsteady flows of the non-aerodynamically loaded system in response to a prescribed perturbation. The staggered phase-modulation signal is applied to prescribe the generalised displacement. Each one of the structural modes used is excited at about its natural frequency and with a phase lag with the preceding mode. The staggered inputs method[6] allows training data to be computed in one single run of CAE computation, achieving greater time saving. The present reduced-order modeling technique is based on the Hammerstein model and correlation method[7]. While the aerodynamic model can be identified by ROM, the structural model is identified independently by using finite-element analysis. The computed aerodynamic model and structure model are coupled to form the closed-loop aeroelastic model, to which eigen-analysis can be applied to determine the flutter boundaries.

While the CAE techniques and ROM method used in this work will be briefly dicussed herein, the main focus of this paper will be on verifying the present numerical scheme. Verification study was performed using the AGARD 445.6 wing. The computational aeroelastic results obtained were compared against experimental data. The Mach numbers considered correspond to those in the experiments. Computations were performed for flow conditions at two different angles of attack $\alpha = 0°$ and $4°$.

Modeling of Flutter Dynamics

Aerodynamic flutter is a closed-loop interaction between air flow and flexible structure. The air movement exerts aerodynamic forces on the structure, which reacts by deforming. This deformation results in a time-varying boundary of the flow domain and, thus, a feedback mechanism between the structural dynamics and aerodynamics. Figure 1 depicts the schematic of a closed-loop aeroelastic system. The aeroelastic equations of

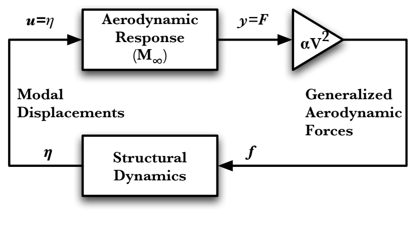

Figure 1. Flutter dynamic system.

motion can be expressed in modal coordinates as

$$\ddot{\eta}_i + 2\zeta_i\omega_i\dot{\eta}_i + \omega_i^2\eta_i = f_i, \qquad i = 1,...,N \qquad (1)$$

where η is the structure modal or generalized displacement, f the generalized aerodynamic forces, N the number of structural modes, and ζ and ω the damping factor and natural frequency, respectively.

The aerodynamic force vector $\boldsymbol{F}$ exerted by the air movement is a nonlinear function of the fluid state vector $\boldsymbol{U}$ and the kinematic boundary conditions as defined by the displacement vector $\boldsymbol{\xi}$ of the flow domain:

$$\boldsymbol{F} = \boldsymbol{F}\left(\boldsymbol{U}, \xi, \dot{\xi}\right), \tag{2}$$

whereas the fluid state vector $\boldsymbol{U} = (\rho, \rho\boldsymbol{v}, \rho E)$, of density ρ, fluid momentum $\rho\boldsymbol{v}$ and total energy ρE, is determined by the solution of the flow governing equation. For this study, the Euler equation is employed for modeling three-dimensional inviscid unsteady flow, which can be expressed in integral form as

$$\frac{\partial}{\partial t}\int_{\Omega(t)} \boldsymbol{U}\, d\Omega + \int_{\partial\Omega(t)} \boldsymbol{\mathcal{F}} \cdot \boldsymbol{n}\, d\sigma = 0, \tag{3}$$

where $\boldsymbol{\mathcal{F}}$ is the flux vector, $\Omega(t)$ is the flow domain with boundary $\partial\Omega(t)$, and $\boldsymbol{n}$ denotes the outward normal vector on the boundary. The flow domain and its boundary are time-varying due to structural deformation. The relation between $\boldsymbol{\xi}$ and $\boldsymbol{\eta}$ is determined by a mapping $\Phi : \boldsymbol{\xi} = \Phi\boldsymbol{\eta}$, called the fluid-structure coupling, which transforms modal displacements into flow domain displacements. Hence, one can write:

$$\Omega(t) = \Omega(\boldsymbol{\eta}(t)), \qquad \partial\Omega(t) = \partial\Omega(\boldsymbol{\eta}(t)). \tag{4}$$

The numerical methods employed for solving the system of equations (2) – (4) consist of a Cartesian grid-based Euler solver using a time-accurate second-order implicit scheme and multigrid procedure to accelerate convergence, and an algebraic transformation for the fluid-structure coupling operator [5]

Equations (2) – (4) describe the aeroelastic response as an N-input, N-output system, with the input being the modal displacements $\boldsymbol{\eta}$, and output being the aerodynamic forces $\boldsymbol{F}$ in modal coordinates. Solution is obtained at a given free-stream Mach number M_∞. The generalized aerodynamic force vector $\boldsymbol{f}$ acting on the structure is related to $\boldsymbol{F}$ by

$$\boldsymbol{f} = \alpha V^2 \boldsymbol{F} \tag{5}$$

where α is a constant depending on the dimensions and mass of the wing, and V is the *speed index* given by

$$V = \frac{V_\infty}{b_s \omega_\alpha \sqrt{\bar{\mu}}}, \tag{6}$$

where V_∞ is the free-stream velocity, b_s is the semi-chord length, ω_α is the natural frequency of wing in first uncoupled torsion mode, and $\bar{\mu}$ is the wing-air mass ratio. The smallest value V_f of V such that the closed-loop is unstable is called the *flutter speed index*, and the frequency ω_f of oscillation is the *flutter frequency*. The traditional definition of *flutter boundaries* are thus the graphs $V_f(M_\infty)$ and $\omega_f(M_\infty)$ [11].

Hammerstein Reduced-Order Model for Flutter Dynamics

The above dynamical system of aeroelastic response has no analytical model, and flutter analysis by full-order simulation is computationally expensive. A faster, system-theoretic method consists in obtaining a reduced-order model of this system. Since aerodynamic response can be regarded as weakly nonlinear under small modal displacement, the Hammerstein model is a suitable choice for ROM.

The ROM technique used in the paper is based on the Correlation Method for Hammerstein System Identification (CMHSI)[7]. Reduced-order aerodynamic model is obtained by identification of the Hammerstein model parameters using input and output data computed in full-order CAE computations. The Hammerstein model is composed of a static nonlinearity $\mathcal{N}[\cdot]$ followed by a linear block represented by its impulse response function $h(\tau)$, as shown in figure 2, where the nonlinearity $\mathcal{N}[\cdot]$ is assumed to take an odd-polynomial form,

$$\begin{aligned} y(t) &= h(\tau) * x(t) \\ &= h(\tau) * \mathcal{N}[u(t)] \\ &= h(\tau) * [\gamma_1 u(t) + \gamma_2 u^3(t) + \cdots + \gamma_p u^{2p+1}(t)]. \end{aligned} \tag{7}$$

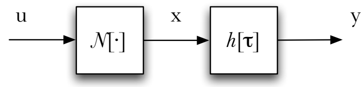

Figure 2. Hammerstein model for aerodynamic response.

Determination of Flutter Boundary via Closed-Loop Eigenvalue Analysis

By adopting the ROM approach, the flutter dynamics of figure 1 is approximated by a closed loop formed by the Hammerstein ROM and the structure model. As aerodynamic is parametrized by free-stream velocity and attack angle, a ROM is obtained for each flow condition. Thus, at each Mach number M and attack angle α, an (M, α, V_f)-parametrized closed-loop model can be constructed. Here, the linear structural dynamics are represented by their transfer-function matrix $G_s(s)$.

For a fixed flow condition defined by M and α, the onset of flutter corresponds to the appearance (if any) of a limit cycle due to bifurcation as the remaining parameter, the speed index V_f, varies. To determine the condition of limit cylce, the Hopf bifurcation theorem states that:

Theorem 1. *For a one-parameter family of nonlinear differential equations $\dot{x} = f_\mu(x)$, there exists a limit cycle for $\mu > \mu_0$ if a pair of eigenvalues of the linearized equation at its equilibrium crosses the imaginary axis from the left-half complex plane to the right-half.*

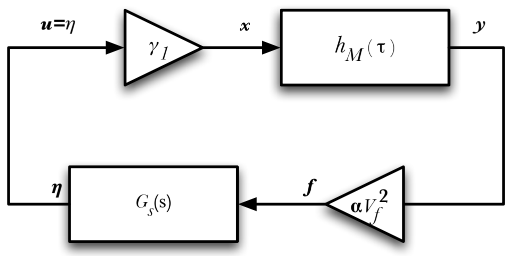

Figure 3. Linearized closed-loop model of flutter dynamics.

In the context of the current study, the family of nonlinear differential equations is that of the reduced-order flutter closed loop parametrized by V_f. It is important to note that, once the ROM is identified, the closed loop is analytical. Moreover, at zero equilibrium $(u = 0, y = 0)$, the linearized equation is simply that of the closed loop with only the linear part of $\mathcal{N}_M$, i.e.

$$x(t) = \gamma_1 u(t), \tag{8}$$

as shown in figure 3. Hence, flutter boundary determination amounts to calculating V_f at which a first pair of eigenvalues crosses the imaginary axis. This can be easily achieved via line search. The crossing frequency is thus the flutter frequency.

Results and Discussion

Computed flutter characteristics of the AGARD 445.6 wing are presented here. The AGARD 445.6 wing was flutter tested in the Transonic Dynamics Tunnel, at Mach numbers from 0.4 to 1.14 at zero-degree angle of attack. Experimental results[11] from this test have been widely used for computational aeroelastic benchmarking. The AGARD wing planform has a quarter-chord sweep angle of 45°, an aspect ratio of 1.65, a taper ratio of 0.66, and a symmetric airfoil. The wing model and structural model used in the present work are depicted in figure 4. Five dominant structural modes of the wing, figure 5, are used. Their natural frequencies are

$$\omega_i = (60.32,\ 239.8,\ 303.8,\ 575.1,\ 742.0)\ \text{rad/sec.}$$

Mode 2 is the first uncoupled torsion mode. That is, $\omega_\alpha =$ 239.8 rad/sec. The structural damping is assumed to be zero, which corresponds to the 'weakened' 2.5-foot panel-span model described in Yates[11]. In order to compare with experimental data, four Mach numbers are investigated:

$$M_\infty = (0.5,\ 0.678,\ 0.90,\ 0.96).$$

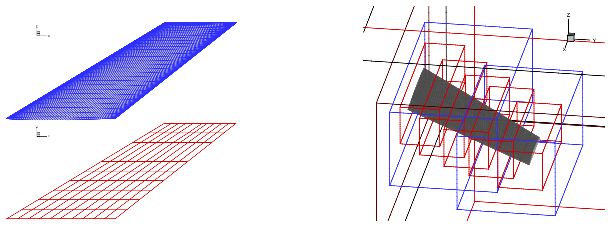

(a) Model of AGARD 445.6 wing

(b) Multi-level Cartesian grids

Figure 4. Numerical models and computational grids for AGARD wing configuration.

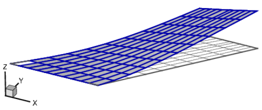

(a) Mode 1, $f_1 = 9.60$Hz

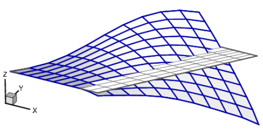

(b) Mode 2, $f_2 = 38.17$Hz

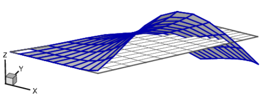

(c) Mode 3, $f_3 = 48.35$Hz

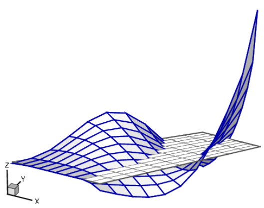

(d) Mode 4, $f_4 = 91.54$Hz

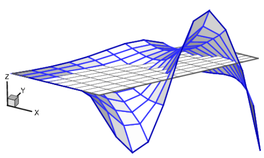

(e) Mode 5, $f_5 = 118.10$Hz

Figure 5. Modal shapes and frequencies of the AGARD 445.6 wing (weakened model).

Determination of flutter boundaries using CAE simulation usually follows the bisection approach. Computations are performed at different speed indices at a fixed Mach number and attack angle. The aeroelastic response in the form of time-varying generalised variables is computed, from which the damping ratio is computed using the logorithmic decrement method. A positive damping ratio signifies stable condition, while negative damping ratio indicates unstable condition. As an example of stable flutter response, the computed generalised displacement at Mach number M_∞ = 0.90 at sub-critical speed index V=0.2 is shown in figure 6. The system exhibits damped oscillation that the generalised displacement decays gradually and progressively after an initial disturbance. As the speed index is increased to V=0.32, the generalised displacement exhibits slightly undamped oscillation. It can be determined from these results that the flutter speed index V_f for M_∞ = 0.90 is at about 0.32.

In the present ROM-based approach, a Hammerstein reduced-order aerodynamic model is first computed using aeroelastic responses obtained by full-order CAE simulation. In this computation the generalised displacement is prescribed by a phase-modulation function

$$a(t) = A\,sin(\omega_c t - \frac{\Delta\omega}{\omega_s} sin(\omega_s t)) \quad , \tag{9}$$

where A is the amplitude, ω_c the central frequency, ω_s the sweep ferquency, and $\Delta\omega$ the frequency semi-band. The parameters of this phase modulation signal are chosen in such a way that the signal covers adequately the required range for the five natural frequencies of the wing. The prescribed generalised displacement and computed generalized aerodynamic forces (GAFs) for a typical case are shown in figure 7. Following the CHMSI method and stability analysis, we obtained the critical speed indices and critical frequencies for the Mach numbers considered. The computed flutter boundaries is compared with experimental results[11] in figure 8. The computational results are in good agreement with experimental results across the Mach number range considered.

The CMHSI method was also exercised to investigate the flutter behavior of the AGARD 445.6 wing at angle of attack $\alpha = 4°$. The solution, shown in figure 7, shows that the critical speed index is reduced slightly as the attack angle is increased from $\alpha = 0°$ to $4°$. This is probably due to an increase in aerodynamic forces as attack angle increases that triggers aeroelastic instability to occur at a lower speed index.

Conclusions

A modeling and simulation framework for flutter analysis has been developed using a combination of full-order computational aeroelasticity techniques and reduced-order modeling methods. Flutter analyses were performed for the AGARD 445.6 wing as part of the validation process. Results showed that the ROM-based predictions matched the experimental data well. The computed flutter speed indices and flutter frequencies showed very satisfactory results.

Acknowledgements

The authors would like to acknowledge support from the FSTD via program agreement 9010102931.

References

[1] Ballhaus, W. F. and Goorjian, P. M., Computation of unsteady transonic flows by the indicial method, *AIAA Journal*, **16**, 1978, 117–124.

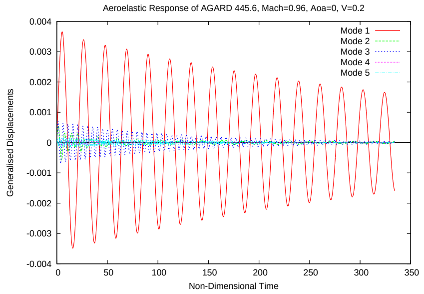

(a) Aeroelastic response at sub-critical state, $M_\infty = 0.96$, $V = 0.2$

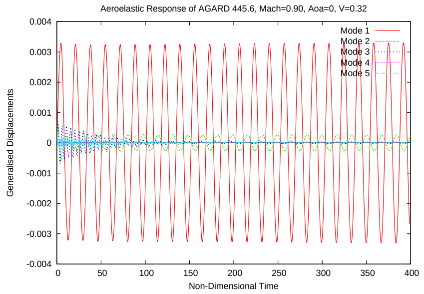

(b) Aeroelastic response near critical state, $M_\infty = 0.90$, $V = 0.32$

Figure 6. Typical aeroelastic response of AGARD 445.6 wing a) at sub-critical, and b) near critical aeroelastic state.

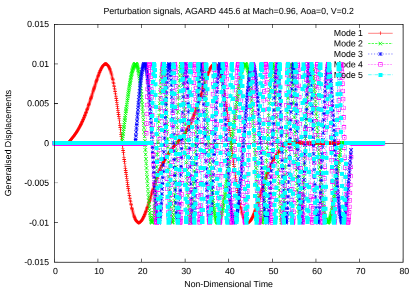

(a) Phase modulation signals

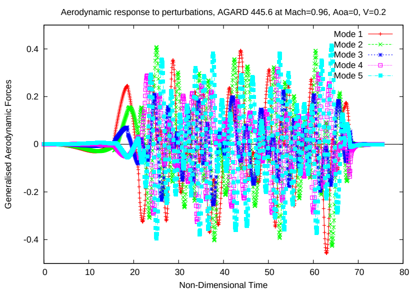

(b) Computed GAF outputs

Figure 7. Input-output data obtained by phase-modulation signals for Hammerstein model identification.

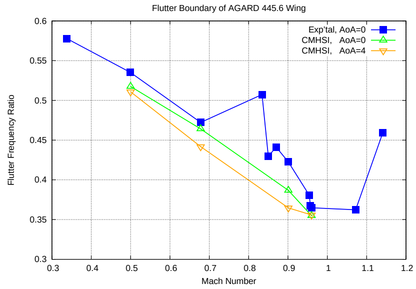

(a) Flutter frequency ratio ω_f/ω_α

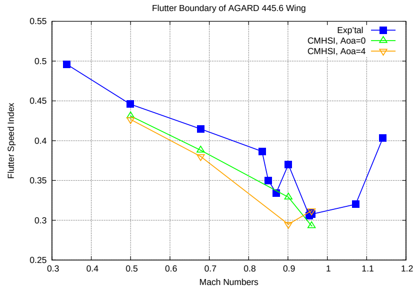

(b) Flutter speed index V_f

Figure 8. Modeled and experimental flutter boundaries of the AGARD 445.6 wing. –▽–: CMHSI, $\alpha = 4°$; –△–: CMHSI, $\alpha = 0°$; –■–: Experimental data, $\alpha = 0°$.

[2] Cowan, T. J., Arena, A. S. and Gupta, K. K., Accelerating computational fluid dynamics based aeroelastic predictions using system identification, *Journal of Aircraft*, **38**, 2001, 81–87.

[3] Dowell, E. H. and Hall, K. C., Modeling of fluid-structure interaction, *Annual Review of Fluid Mechanics*, **33**, 2001, 445–490.

[4] Hamel, P. G. and Jategaonkar, R. V., Evolution of flight vehicle system identification, *Journal of Aircraft*, **33**, 1996, 9–28.

[5] Lai, K. L., Koh, E. P. C. and Tsai, H. M., Flutter computations of complex configurations using Cartesian grids, in *Proc. 44th AIAA Aerospace Sciences Meeting and Exhibit*, Reno, NV, USA, 2006, AIAA Paper 2006-1399.

[6] Lai, K. L. and Lum, K.-Y., Reduced-order based flutter analysis for complex aeroelastic systems, in *Proc. 26th AIAA Applied Aerodynamics Conference*, Honolulu, HI, USA, 2008, AIAA Paper 2008-6240.

[7] Lum, K.-Y. and Lai, K. L., Identification of a Hammerstein model for wing flutter analysis using CFD data and correlation method, in *Proc. American Control Conference*, Baltimore, MD, 2010, 1314 –1319, 1314 –1319.

[8] Noor, A., Recent advances in reduction methods for nonlinear problems, *Comput. Struct.*, **13**, 1981, 31–44.

[9] Silva, W. A. and Raveh, D. E., Development of unsteady aerodynamic state-space models from CFD-based pulse responses, in *Proc. 42nd AIAA/ASME/ASCE/ASH/ASC Structures, Structural Dynamics, and Materials conference*, Seattle, WA, USA, 2001, AIAA Paper 2001-1213.

[10] Tobak, M., On the use of indicial function concept in the analysis of unsteady motions of wings and wing-tail combinations, Technical Report 1188, NACA, 1954.

[11] Yates, E. C. J., Land, N. S. and Foughner, J. T., Measured and calculated subsonic and transonic flutter characteristics of a 45° sweptback wing planform in air and in Freon-12 in the Langley Transonic Dynamics Tunnel, Technical Report TN D-1616, AGARD, 1963.